Chemical Engineering Journal 144 (2008) 329–335

Contents lists available at ScienceDirect

Chemical Engineering Journal

journal homepage: www.elsevier.com/locate/cej

Preparation of kerosene-based magnetic fluid under microwave irradiation via phase-transfer method

R.Y. Hong[a,b,*], B. Feng[a], Z.Q. Ren[a], B. Xu[c], H.Z. Li[b], Y. Zheng[d], D.G. Wei[e]

[a] Chemical Engineering Department & Key Laboratory of Organic Synthesis of Jiangsu Province, Soochow University, SIP, Suzhou 215123, China
[b] Key Laboratory of Multiphase Reaction, Institute of Process Engineering, Chinese Academy of Sciences, Beijing 100080, China
[c] Nanotec Inc., SIP, Suzhou 215123, China
[d] Department of Chemical Engineering, University of New Brunswick, Fredericton, N.B., E3B 5A3 Canada
[e] Center for Nanoscale Systems, School of Engineering & Applied Science, Harvard University, 11 Oxford Street, Cambridge, MA 02139, USA

ARTICLE INFO

Article history:
Received 9 April 2008
Received in revised form 29 June 2008
Accepted 6 July 2008

Keywords:
Magnetic fluid
Oleic acid
Surface modification
Microwave synthesis

ABSTRACT

Fe_3O_4 magnetic nanoparticles (MNPs) were prepared by the co-precipitation of Fe^{3+} and Fe^{2+} using $NH_3{\cdot}H_2O$ under microwave irradiation to enhance the crystallization of Fe_3O_4 MNPs. The MNPs were formed in the aqueous phase, modified by oleic acid and migrated to the organic phase of kerosene to form a magnetic fluid (MF). The core size of MNPs was found to be around 10 nm by TEM. FT-IR results indicated that a covalent bond was formed between the hydroxyl groups on the surface of MNPs and the carboxyl groups of oleic acid. The MF demonstrated good stability, and had susceptibility of 7.78×10^{-4} and saturation magnetization of 27.3 emu/g. In addition, the mean size of aggregates in MF was 27.51 nm. Finally, the rheological property of the prepared MF was investigated using a rotating rheometer attached with a custom-built solenoid coil. It was found that the MF demonstrated shear-thinning behavior and could be described by the Herschel–Bulkley model.

1. Introduction

A magnetic fluid (MF) is a colloidal suspension of magnetic nanoparticles in a carrier liquid, and the physical properties of MF can be controlled even by a moderate magnetic field [1,2]. This was expected to give rise to numerous new applications, such as electrophotographic developer [3], magnetic separation [4], efficient heat transfer [5], MRI contrast agent [6], and so on. For many of these applications, the preparation of magnetic nanoparticles (MNPs) is of key importance because the properties of MNPs depend strongly on their dimensions. However, due to the large specific surface area, high surface energy and magnetization of MNPs, the MNPs are prone to aggregate. In order to improve the dispersion of MNPs and the compatibility of MNPs with organic solvents, surface treatment for MNPs is a necessity.

A variety of methods have been reported in literature to prepare MF, including high-energy ball milling [7], surface coating [8] and grafting by agent [9], hydrothermal processing [10], ATRP method [11] and micro-emulsion method [12]. Our previous studies [13] have shown that co-precipitation from the solution of Fe^{2+} and Fe^{3+} with aqueous ammonia followed by aging at room temperature was a simple way to obtain Fe_3O_4 MFs with high saturation magnetization. However, the aging is not favorable since the period is too long.

In some circumstances, microwave (MW) irradiation might be a promising method in preparing materials due to the thermal and non-thermal effects of MW. Compared with the conventional methods for synthesizing nanoparticles, MW processing has the advantages of short reaction time, small particle size and narrow size distribution. Recently, phase-transfer method has been reported by several groups [14]. This method can simplify the steps and further manipulate the size and size distribution as well as the morphology of the MNPs. Our group has reported the synthesis of Fe_3O_4 MNPs with better crystalline structure using MW irradiation [15], although the procedures were not simple. In the present investigation, Fe_3O_4 MNPs were aged under MW irradiation, and the oleic-acid-coated Fe_3O_4 MNPs were transferred from water phase to kerosene phase to form a stable MF via a simple one-step phase-transfer method.

2. Experimental

2.1. Materials

Ferric chloride ($FeCl_3{\cdot}6H_2O$), ferrous sulfate ($FeSO_4{\cdot}7H_2O$), aqueous ammonia and oleic acid were all of analytic grade.

* Corresponding author at: Department of Chemical Engineering, Key Laboratory of Organic Synthesis of Jiangsu Province, Soochow University, SIP, Suzhou, Jiangsu 215123, China. Tel.: +86 512 6588 0402; fax: +86 512 6588 0089.
E-mail addresses: rhong@suda.edu.cn (R.Y. Hong), yzheng@unb.ca (Y. Zheng), dougwei@deas.harvard.edu (D.G. Wei).

1385-8947/$ – see front matter © 2008 Elsevier B.V. All rights reserved.
doi:10.1016/j.cej.2008.07.012

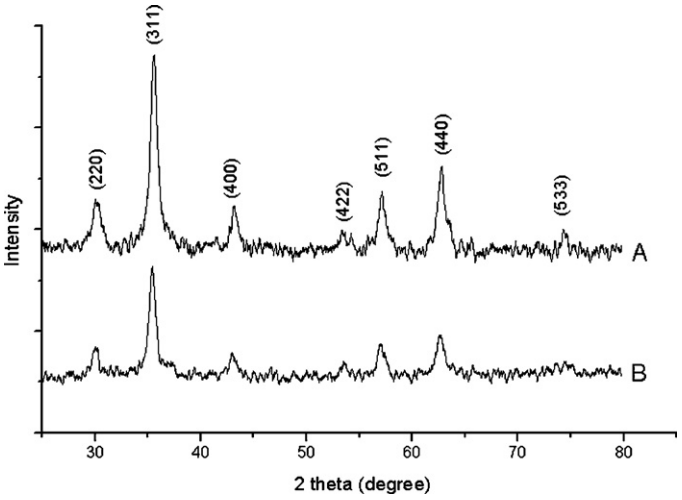

Fig. 1. XRD patterns of Fe_3O_4 MNPs (Samples A and B were prepared with and without MW irradiation, respectively).

Kerosene was of chemical grade. Deionized water was used throughout experiments.

2.2. Preparation of MF

To synthesize Fe_3O_4 MNPs, a mixture of $FeCl_3$ (0.18 mol) and $FeSO_4$ (0.12 mol) was dissolved into 100 mL of deionized water. Then 100 mL of ammonia aqueous solution was dropped into the mixture quickly with violent stirring. Thereafter, the solution was kept stirred for additional 30 min. The resultant black mixture was aged under MW irradiation at a frequency of 2.45 GHz for 1 h. The temperature was kept at 85 °C by setting the mixture in a water bath. Then 5 mL of oleic acid was added to modify the surface of Fe_3O_4 MNPs. The modification reaction was kept for 1 h at a temperature of 95 °C under MW irradiation. Then 100 mL of kerosene was added to the mixture with stirring. The peptization of the oleic-acid-coated MNPs occurred. The mixture was kept at 95 °C under stirring for 1 h and a distinct phase separation occurred between the aqueous and organic portions. After removing the aqueous phase using a pipette, the kerosene-based MF was obtained.

2.3. Characterization

Fourier transform infrared (FT-IR) spectra were obtained using Nicolet FT-IR Avatar 360 with KBr method. The nanoparticles sizes were determined by Hitachi H-600-II transmission electron microscope (TEM) and HITACHI S570 scanning electron microscope (SEM). X-ray diffraction (XRD) measurements were carried out with D/Max-IIIC, using Cu Kα radiation. The magnetic properties of MNPs were measured on a BHV-55 vibrating sample magnetometer (VSM). The thermal stability of oleic-acid-coated MNPs was measured by DSC (PERKIN-ELMER). UV–vis spectra were achieved by HITACHI U-2810 spectrophotometer. The magnetic property of MF was measured by Gouy magnetic balance (FD-TX-FM-A). The size of nanoparticles/aggregates in MF was obtained using Malvern HPPS5001 laser particle-size analyzer.

3. Results and discussion

3.1. X-ray powder diffraction patterns

Fig. 1 shows the X-ray powder diffraction patterns of Fe_3O_4 MNPs that were separated from the MF. Sample A was prepared using MW irradiation, and Sample B was prepared using oil bath. From the patterns of Sample A, it was found that there were a series of characteristic peaks at 2.968 (2 2 0), 2.535 (3 1 1), 2.103 (4 0 0), 1.719 (4 2 2), 1.614 (5 1 1), 1.478 (4 4 0) and 1.271 (5 3 3). The d values of Sample A calculated from the XRD patterns were well indexed to the inverse cubic spinel phase of Fe_3O_4; this is accordance with the IR results in Section 3.4. The average crystallite size D was obtained from Sherrer equation: $D = K\lambda/(\beta \cos \theta)$, where K is a constant ($K = 0.9$ for Cu Kα), λ is wavelength (0.15405 nm for Cu Kα) and β is the half of the maximum width of the strongest diffraction peak. The crystallite size of Sample A was about 9 nm. The patterns of Sample B were similar to those of Sample A, and the average size of Sample B was about 10 nm. However, the intensity of Sample A was higher than that of Sample B. It indicated that Sample A had more complete crystalline structure than that of Sample B. This suggested that MW irradiation could remarkably improve the crystalline structure of Fe_3O_4 MNPs.

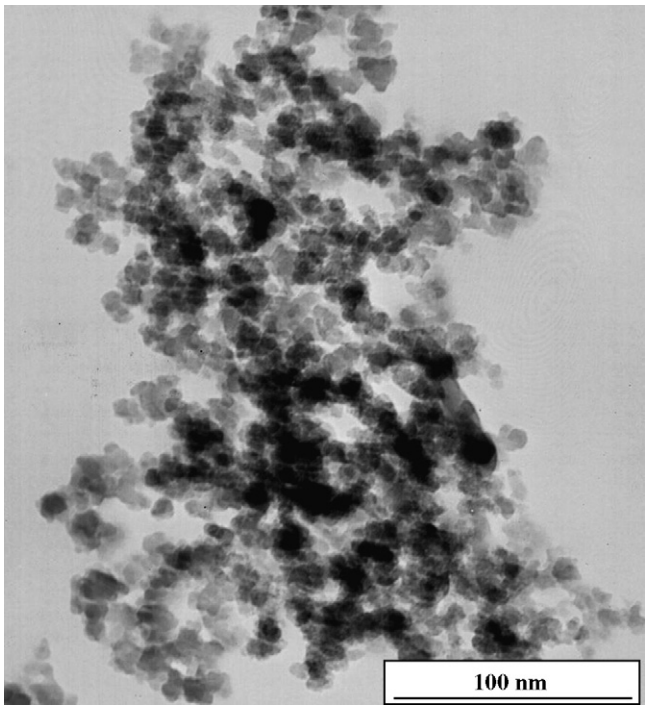

Fig. 2. TEM of Fe_3O_4 MNPs.

3.2. TEM and SEM images

Fig. 2 shows the TEM image and Fig. 3 shows the SEM image of Fe_3O_4 MNPs in kerosene-based MF prepared under MW irradiation. The TEM and SEM photographs illustrated that the normal size of Fe_3O_4 MNPs was about 9 nm, slightly smaller than that aged for 7 days, which matched the results obtained from XRD. The average size of the samples aged for 7 days was found to be about 10 nm [13]. However, some of the MNPs congregated because of the large specific surface area, high surface energy and magnetism of Fe_3O_4 MNPs [16].

3.3. Hysteresis cycle of MNPs

The magnetic properties of Fe_3O_4 MNPs prepared under two different conditions were characterized by a VSM at room temperature. As shown in Fig. 4, both samples are superparamagnetic and the saturation magnetization (Ms) of Sample A prepared using MW

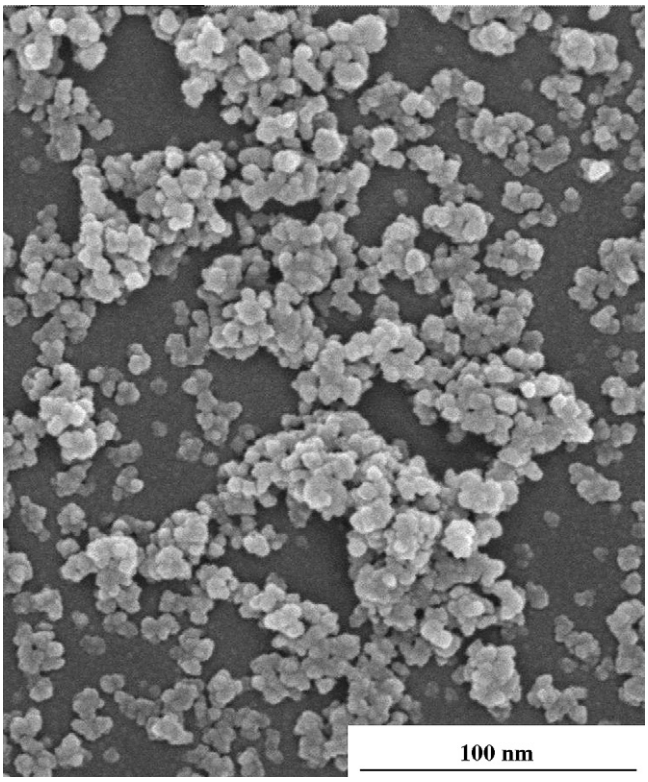

Fig. 3. SEM of Fe_3O_4 MNPs.

is 75.32 emu/g, which is higher than that of Sample B (63.28 emu/g) prepared using oil bath. After studying the XRD patterns of two samples, we find that the Ms increased with the improvement of crystallinity. The particle size has been reported to influence the magnetic properties of materials. However, the particle size should not influence too much the saturation magnetization of Samples A and B for they almost have the same crystallite size. The phenomenon is related to the difference in crystallinity. The well-crystallized particles have a thinner non-magnetic surface layer and less superparamagnetic relaxation, which can explain the increase of saturation magnetization. Better crystallinity in Fe_3O_4 MNPs would result in less crystal defects. Therefore, the superexchange interaction of Fe–O–Fe was strengthened, and the magnetic properties of Fe_3O_4 MNPs were improved.

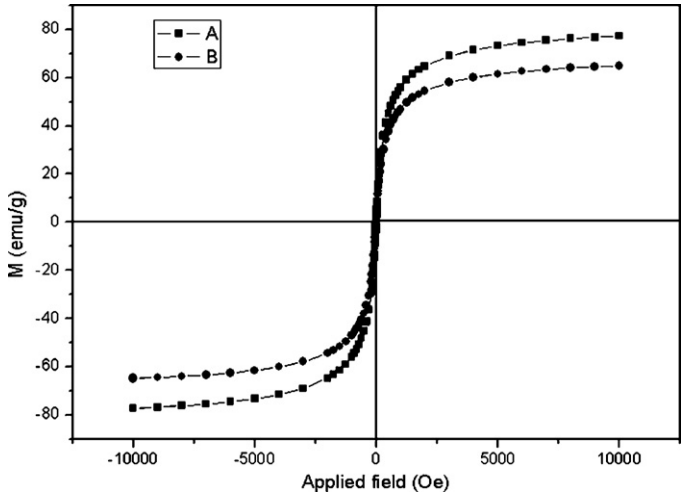

Fig. 4. Magnetic hysteresis curves of Fe_3O_4 MNPs (Samples A and B were prepared with and without MW irradiation, respectively).

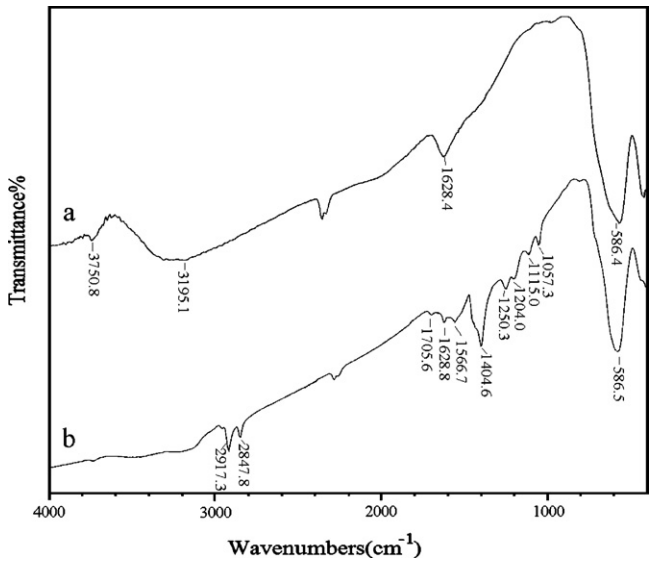

Fig. 5. FT-IR spectra of (a) bare Fe_3O_4 MNPs; (b) oleic-acid-coated Fe_3O_4 MNPs.

The cocercivity of the MNPs aged under MW irradiation is about 6.78 Oe, which is much higher than the value of 3.74 Oe of the MNPs synthesized using the conventional co-precipitation method. This could be ascribed to the reduction of size of Fe_3O_4 nanoparticle.

3.4. FT-IR spectra

Fig. 5(a) is the FT-IR spectrum of bare Fe_3O_4 MNPs. As can be seen, a broad band exists at around 586.4 cm^{-1}, assignable to the Fe–O of the magnetite [17]. From the IR analysis, it is evident that the as-prepared nanoparticles are Fe_3O_4. Fig. 5(b) shows the IR spectrum of Fe_3O_4 MNPs coated with oleic acid. It can be seen from Fig. 5(b) that the possessed absorption band in 586.5 cm^{-1} is due to stretching vibration of Fe–O bond of Fe_3O_4. By comparing with Fig. 5(a), some new absorption peaks are found in Fig. 5(b). The characteristic absorption peaks of $-CH_3$ are observed at 2959.0 and 1385.0 cm^{-1}. The absorptions at 2917.3 and 2847.8 cm^{-1} were characteristic for the stretching vibration of CH_2, in addition, the peak at 1057.3 cm^{-1} representing stretching vibration of –C=C– bond. In addition, the two peaks at 1628.8 and 1404.16 cm^{-1} are due to the symmetric and asymmetric carboxylate (COO–) stretch, respectively [18]. It revealed that oleic acid has been successfully grafted onto the surface of Fe_3O_4 MNPs through the reaction of hydroxide radical groups on the surface of Fe_3O_4 MNPs with carboxyl groups of oleic acid, similar to the etherification. The reaction mechanism is illustrated in Fig. 6.

3.5. Thermal analysis

Fig. 7 shows the TGA curve of the MNPs obtained by drying MF. The sample was measured through the TGA runs in the condition of nitrogen atmosphere at the heating rate of 15 °C/min. The organic materials and magnetite of the samples are completely burned to gas and converted to iron oxides at the elevated temperature (say higher than 500 °C), respectively [19]. There were two stages of degradation, as shown in the TGA curve. The first-stage weight loss which occurred near 250 °C was due to the evaporation of oleic acid which was absorbed by physical bond on the surface of MNPs, and oleic acid would completely decompose when the temperature reaches about 400 °C, as shown in Fig. 7 [20]. While the

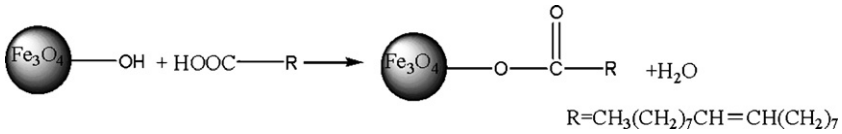

Fig. 6. The reaction of Fe_3O_4 MNPs and oleic acid.

second-stage weight loss occurred at about 400 °C, was due to the degradation of CH–O–Fe. This was in accordance with Ref. [21].

3.6. Stability of MF

The UV–vis spectrum of MF under gravitation field for 60 days and heated for 12 h at 100 °C is presented in Fig. 8(a). The absorbance of MF was almost never changed after sedimentation for 60 days or heating at 100 °C for 12 h and the MF was proved to have good stability.

It is very important to prepare MFs, which are still stable after being diluted. Fig. 8(b) shows the visible spectrum of the diluted MF under gravity for 60 days. The sample was diluted with kerosene at the ratio of 1:50, respectively. Minor absorbance change was noted. Such a change was due to the reaction between hydroxide radical groups on the MNPs surface with carboxyl groups of oleate sodium. When the MF was diluted, the surface layers of the colloid could not be destroyed. Therefore, the MF demonstrates good stability, even after being diluted.

Another important requirement of MF is that it is still stable under intense magnetic field. In the present investigation, a MF with a weight concentration of 20% was put under the magnet field with the intensity of 13.6 mT. The relationship between time and magnetic weight is shown in Fig. 9. The magnetic weights almost have no difference after sedimentation under the magnet field for 24 h. The MF was proved to have good stability under magnet field.

3.7. Particle size distribution in MF

Fig. 10(a) shows the size distribution of oleic-acid-treated Fe_3O_4 MNPs or aggregates dispersed in MF, which was newly prepared. The diameter of the MNPs was 27.51 nm, which means the median size of 99% particles in volume was 27.51 nm. Fig. 10(b) shows the MF that was set for sedimentation under gravity for 60 days. The diameter of the MNPs was 29.32 nm. By comparing Fig. 10(b) with (a), we found that the diameters have little differences between the newly prepared MF and the one after sedimentation for 60 days. This means the Fe_3O_4 MNPs dispersed in MF has good stability and this result was accordance with the UV–vis analysis.

The core size of MNPs obtained from TEM was about 10 nm, which were smaller than that of MNPs/aggregates in MF. An explanation for this is that some of the primary nanoparticles aggregated in MF in spite of particles coated by oleic acid.

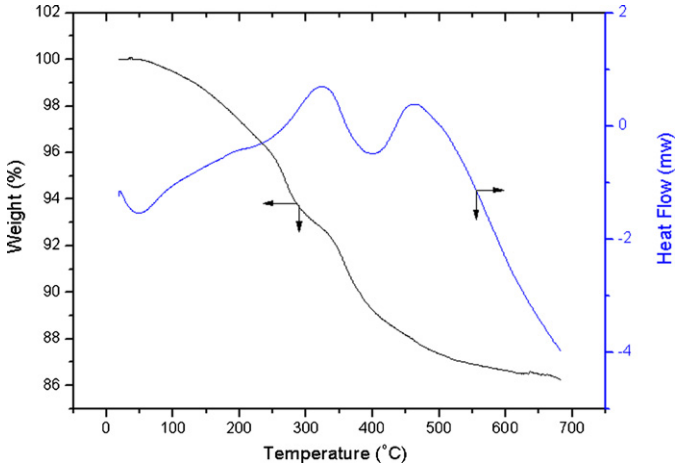

Fig. 7. DSC–TGA curves of oleic-acid-coated MNPs.

3.8. Magnetic property of MF

The susceptibility and saturation magnetization are very important properties of MF. In the present investigation, a MF with a weight concentration of 20% was prepared. The relationship between the magnetic weight and applied magnetic field for the MF was shown in Fig. 11. According to the calculation method presented in literature [22], the saturation magnetization and susceptibility were 1.44×10^5 A/m and 7.78×10^{-4}, respectively, which is much higher than that prepared using traditional method [13].

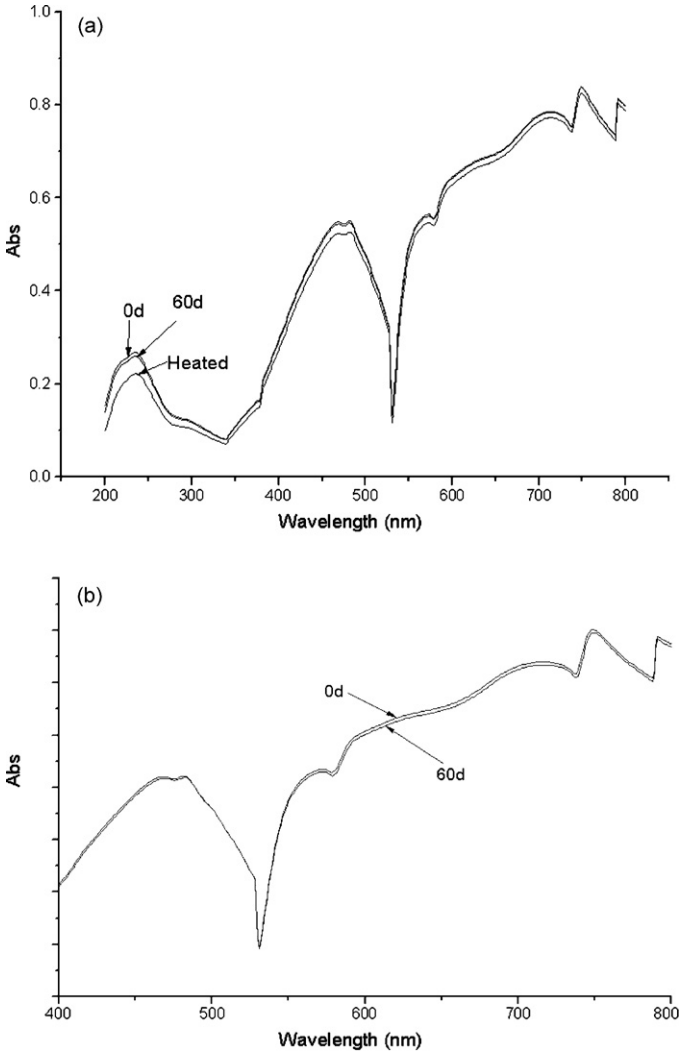

Fig. 8. UV–vis spectrum of MF set under gravity for 60 days (a) original MF; (b) diluted MF.

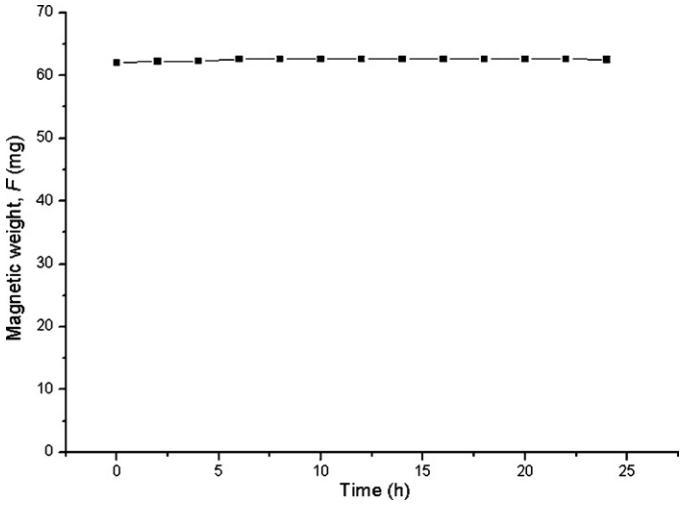

Fig. 9. Relationship between time and magnetic weight (H = 13.6 mT).

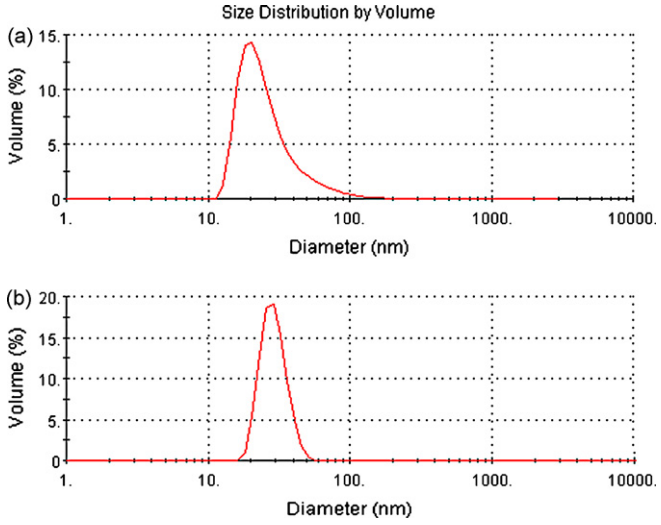

Fig. 10. Particle size distribution in MF.

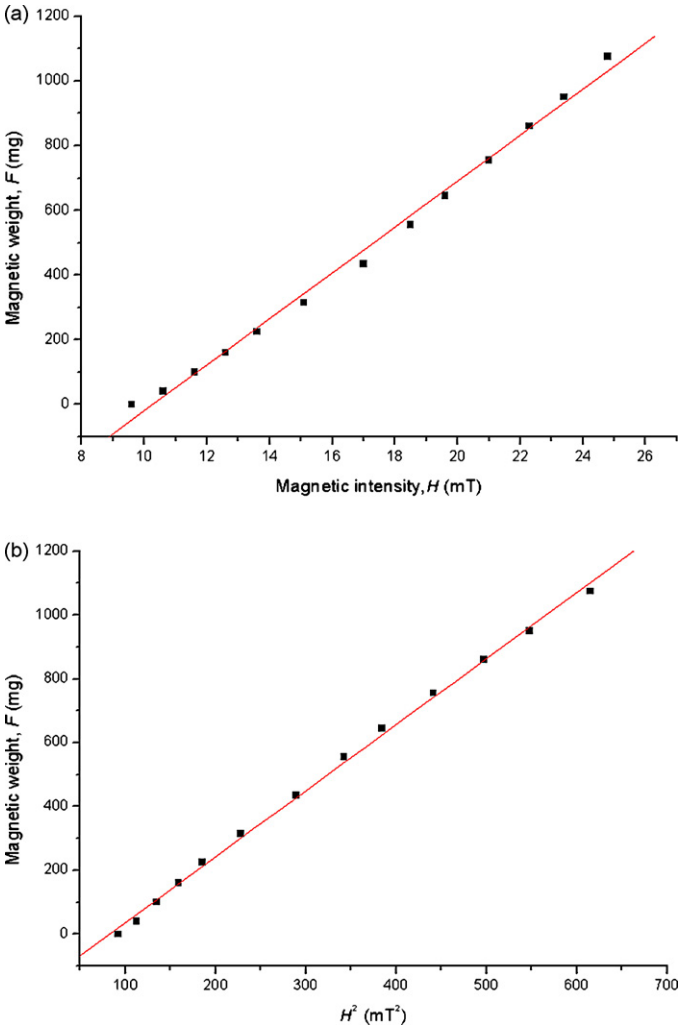

Fig. 11. Relationship between magnetic weight and magnetic field intensity.

3.9. Rheological property of MF

In this section, four samples with different solid contents were prepared. Sample 1 with solid content 20% was prepared using the method presented in Section 2.2. Other samples were obtained by diluting Sample 1 gradually.

The rheological properties of MFs were measured using a rotating rheometer (Brookfield LVDV III+) attached to a custom-built solenoid coil. Fig. 12 shows the schematic diagram of the measuring system. The experimental results were analyzed using Rheocalc

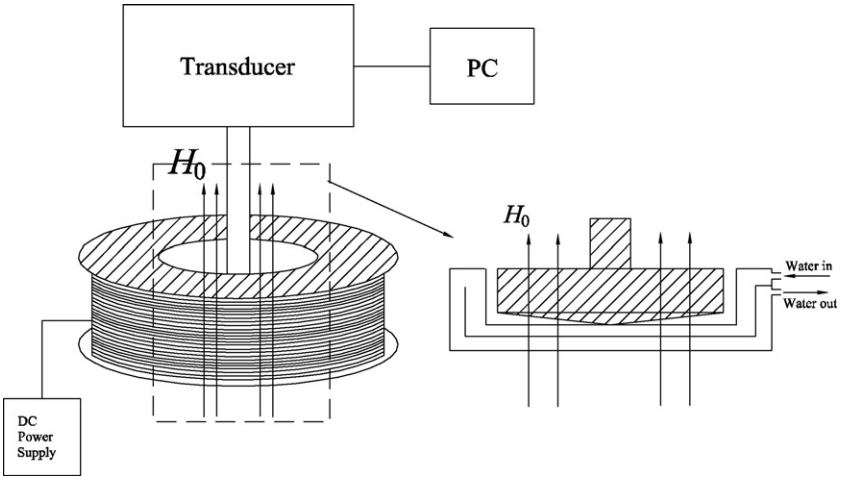

Fig. 12. A rotating rheometer for measuring viscosity under applied magnetic field.

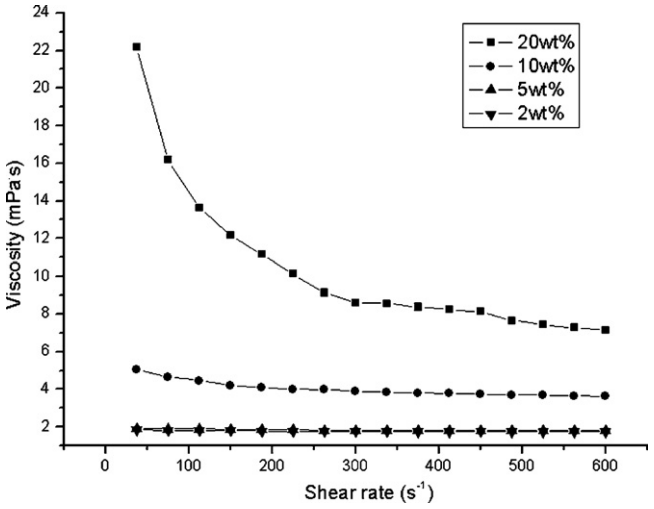

Fig. 13. Viscosity versus shear rate under different solid contents.

V2.7 (software of Brookfield [23]). The magnetic filed perpendicular to the shear flow was generated by the solenoid surrounding the spindle. The intensity of magnetic field was measured using a Hall-effect sensor. A thermostatic chamber was used to supply water to control the temperature of MFs during measurements. The spindle, CEP-52, of the rotating rheometer was chosen. The torque during the experimental measurements was kept within 10–90% of the maximum torque. 0.5 mL of MFs was used for every measurement.

3.9.1. Shear-thinning behavior

When the shear rate increases, there are three kinds of variations for the viscosity of any soft matter: Newtonian, shear-thinning and shear-thickening. Fig. 13 shows that the MF with relative high solids contents demonstrates the shear-thinning behavior without the applied magnetic field.

Fig. 14 demonstrates similar trend as that of Fig. 13. The shear-thinning behavior is also observed when there is an applied magnetic field. Moreover, the shear-thinning behavior becomes even obvious as the intensity of applied magnetic field increases.

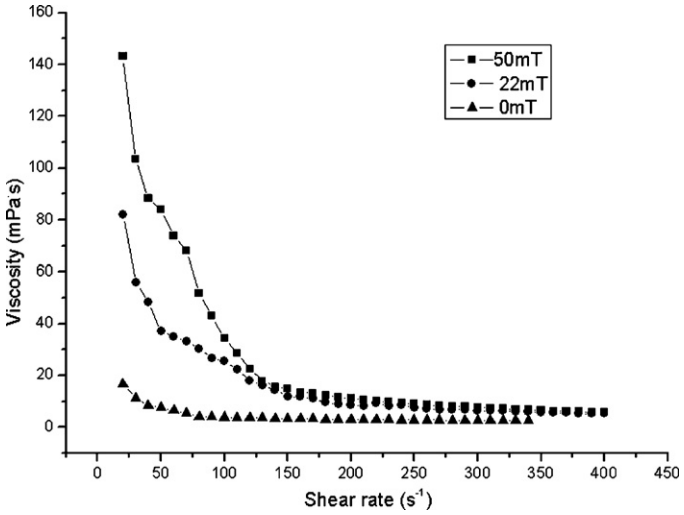

Fig. 14. Viscosity versus shear rate under applied magnetic field.

Table 1
Analyzed results using Herschel–Bulkley model without magnetic field

	Solid content (wt%)			
	2	5	10	20
Viscosity, η (mPa s)	1.60	2.36	5.94	20.3
Yield stress, τ_0 (Pa)	0.02	0.10	0.30	0.65
Shear-thinning exponent, n	1.0	0.98	0.92	0.85
Correlation coefficient (%)	100.0	100.0	100.0	99.8

Table 2
Analyzed results using Herschel–Bulkley model under magnetic field (20 wt%)

	Magnetic field intensity (mT)		
	0	22	50
Viscosity, η (mPa s)	20.3	82.5	150.2
Yield stress, τ_0 (Pa)	0.65	2.41	5.22
Shear-thinning exponent, n	0.85	0.80	0.79
Correlation coefficient (%)	99.8	95.4	93.2

3.9.2. Constitutive equations for MFs

Some researchers found that the rheological properties of MF under applied magnetic field could be described using the Bingham model. Our previous studies [1] showed that the characteristics of MFs gradually deviated from the Bingham model when the intensity of applied magnetic field increased. The Herschel–Bulkley model is recommended to describe shear-thinning behavior of MFs both with and without magnetic field. In this study, correlation was made for the experimental data using the Herschel–Bulkley model and the correlated parameters are listed in Tables 1 and 2. The parameters of other constitutive equations were omitted for the sake of simplicity. It can be seen that the Herschel–Bulkley equation is the best one describing the shear stress of MFs with and without the application of magnetic field.

3.9.3. Viscosity versus magnetic field intensity

The measured viscosity of MFs under magnetic field is illustrated in Fig. 14. By comparing the curves, it is found that the applied magnetic field had an obvious effect on the viscosity of MFs. The result from Fig. 14 is in accordance with our previous studies [1] and the trend revealed by Table 2. Since the viscosity of kerosene was not affected by an applied magnetic field, the viscosity of MFs is determined by the properties of MNPs. Under magnetic field, MNPs are polarized and arrange their orientation along the direction of magnetic field. The augment of magnetic field intensity increases the interaction among MNPs, and the flow resistance increases. Finally, it shows that viscosity of MFs increases with the increase of magnetic field. The stronger the intensity of magnetic field, the larger the viscosity. The arranged microstructure of MFs is destroyed gradually with the increase of shear rate. Thus, the viscosity of highly concentrated MFs decreases quickly as the increasing shear rate.

4. Conclusions

The following conclusions can be drawn in the present investigation.

(1) Fe_3O_4 MNPs prepared under MW irradiation have more complete crystalline structure and hence have higher saturation magnetization than those prepared under ordinary conditions.
(2) Oleic acid was successfully introduced onto the surface of Fe_3O_4 MNPs. The kerosene-based Fe_3O_4 MF was prepared using aqueous to kerosene phase-transfer method. The prepared MF showed good stability. The susceptibility of MF was 7.78×10^{-4}

and the saturation magnetization was 27.3 emu/g. In addition, the mean size Fe_3O_4 MNPs in the MF was 27.51 nm.

(3) The viscosity of Fe_3O_4 MFs increased obviously with the increasing intensity of magnetic field. The shear stress versus shear rate of MFs could be described by the Herschel–Bulkley model whether MFs were subject to applied magnetic field or not.

Acknowledgments

This project was supported by the National Natural Science Foundation of China (NNSFC, nos. 20476065 and 20736004), the Scientific Research Foundation for the ROCs of State Education Ministry (SRF for ROCS, SEM), the Key Laboratory of Multiphase Reaction of the Chinese Academy of Science (no. 2006-5), the State Key Laboratory of Coal Conversion of CAS (no.2006-902), the Key Laboratory of Organic Synthesis of Jiangsu Province, the Chemical Experiment Center of Soochow University and R&D Foundation of Nanjing Medical University (NY0586).

References

[1] R.Y. Hong, Z.Q. Ren, Y.P. Han, et al., Rheological properties of water-based Fe_3O_4 ferrofluids, Chem. Eng. Sci. 62 (2007) 5912–5924.
[2] P.C. Fannin, Characterisation of magnetic fluids, J. Alloy Compd. 369 (2004) 43–51.
[3] Y.B. Khollam, S.R. Dhage, H.S. Potdar, Microwave hydrothermal preparation of submicron-sized spherical magnetite (Fe_3O_4) powders, J. Magn. Magn. Mater. 56 (2002) 571–577.
[4] P.A. Augusto, T.C. Grande, P. Augusto, Magnetic classification in health sciences and in chemical engineering, Chem. Eng. J. 111 (2005) 85–90.
[5] K. Nakatsuka, B. Jeyadevan, S. Neveu, The magnetic fluid for heat transfer applications, J. Magn. Magn. Mater. 252 (2002) 360–362.
[6] C.C. Berry, A.S. Curtis, Functionalisation of magnetic nanoparticles for applications in biomedicine, J. Phys. D 36 (2003) 198–206.
[7] L.S. Darken, R.W. Gurry, The system iron-oxygen II equilibrium and thermodynamics of liquid oxide and other phases, J. Am. Chem. Soc. 68 (1946) 798–816.
[8] Z.F. Wang, B. Shen, Z. Aihua, N.Y. Hea, Synthesis of Pd/Fe_3O_4 nanoparticle-based catalyst for the cross-coupling of acrylic acid with iodobenzene, Chem. Eng. J. 113 (2005) 27–34.
[9] M. Ma, Y. Zhang, W. Yu, Preparation and characterization of magnetite nanoparticles coated by amino silane, Colloid Surf. A 212 (2003) 219–226.
[10] K. Byrappa, S. Ohara, T. Adschiri, Nanoparticles synthesis using supercritical fluid technology-towards biomedical applications, Adv. Drug Deliv. Rev. 60 (2008) 299–327.
[11] Y. Zhou, S.X. Wang, B.J. Ding, Z.M. Yang, Modification of magnetite nanoparticles via surface-initiated atom transfer radical polymerization (ATRP), Chem. Eng. J. 138 (2008) 578–585.
[12] Y. Chen, Z. Qian, Z.H. Zhang, Novel preparation of magnetite/polystyrene composite particles via inverse emulsion polymerization, Colloid Surf. A 312 (2008) 209–213.
[13] R.Y. Hong, J.H. Li, J. Wang, H.Z. Li, Comparison of schemes for preparing magnetic Fe_3O_4 nanoparticles, Particuology 5 (2007) 186–191.
[14] M.A. Bakar, W.L. Tan, N.A. Bakar, A simple synthesis of size-reduce magnetite nano-crystals via aqueous to toluene phase-transfer method, J. Magn. Magn. Mater. 314 (2007) 1–6.
[15] R.Y. Hong, T.T. Pan, H.Z. Li, Microwave synthesis of magnetic Fe_3O_4 nanoparticles used as a precursor of nanocomposites and ferrofluids, J. Magn. Magn. Mater. 303 (2006) 60–68.
[16] C. Dominika, H. Nübold, Magnetic aggregation: dynamics and numerical modeling, Icarus 157 (2002) 173–186.
[17] R.Y. Hong, T.T. Pan, Y.P. Han, H.Z. Li, J. Ding, S.J. Han, Magnetic field synthesis of Fe_3O_4 nanoparticles used as a precursor of ferrofluids, J. Magn. Magn. Mater. 310 (1) (2007) 37–47.
[18] R.Y. Hong, J.H. Li, H.Z. Li, J. Ding, Y. Zheng, D.G. Wei, Synthesis of Fe_3O_4 nanoparticles without inert gas protection used as precursors of magnetic fluids, J. Magn. Magn. Mater. 320 (2008) 1605–1614.
[19] W.M. Zheng, F. Gao, H.C. Gu, Magnetic polymer nanospheres with high and uniform magnetite content, J. Magn. Magn. Mater. 288 (2005) 403–410.
[20] F. Montagne, O. Mondain-Monval, C. Pichot, A. Elaissari, Highly magnetic latexes from submicrometer oil in water ferrofluid emulsions, J. Polym. Sci. Part A: Polym. Chem. 44 (2006) 2642–2656.
[21] L. Shen, P.E. Laibinis, T.A. Hatton, Bilayer surfactant stabilized magnetic fluids: synthesis and interactions at interfaces, Langmuir 15 (1999) 447–453.
[22] R.E. Rosensweig, Ferrohydrodynamics, Dover Publications, Inc., NY, 1997, pp. 136–137.
[23] Brookfield Inc., Brookfield LVDV III+ programmable rheometer operating instructions, manual no. M/98-211-B0104 (2006).